Immunity, Vol. 22, 19–29, January, 2005, Copyright ©2005 by Elsevier Inc. DOI 10.1016/j.immuni.2004.11.013

The Conduit System Transports Soluble Antigens from the Afferent Lymph to Resident Dendritic Cells in the T Cell Area of the Lymph Node

Michael Sixt,[1,*] Nobuo Kanazawa,[2] Manuel Selg,[1] Thomas Samson,[3] Gunnel Roos,[1] Dieter P. Reinhardt,[4] Reinhard Pabst,[5] Manfred B. Lutz,[2] and Lydia Sorokin[1]

[1]Department for Experimental Pathology
Lund University
22185 Lund
Sweden

[2]Department of Dermatology
University of Erlangen
91052 Erlangen
Germany

[3]Department of Experimental Medicine I
University of Erlangen
91054 Erlangen
Germany

[4]Department of Anatomy and Cell Biology
McGill University
Montreal H3A 2B2
Canada

[5]Department of Functional and Applied Anatomy
Medical School of Hannover
30625 Hannover
Germany

Summary

Resident dendritic cells (DC) within the T cell area of the lymph node take up soluble antigens that enter via the afferent lymphatics before antigen carrying DC arrive from the periphery. The reticular network within the lymph node is a conduit system forming the infrastructure for the fast delivery of soluble substances from the afferent lymph to the lumen of high endothelial venules (HEVs). Using high-resolution light microscopy and 3D reconstruction, we show here that these conduits are unique basement membrane-like structures ensheathed by fibroblastic reticular cells with occasional resident DC embedded within this cell layer. Conduit-associated DC are capable of taking up and processing soluble antigens transported within the conduits, whereas immigrated mature DC occur remote from the reticular fibers. The conduit system is, therefore, not a closed compartment that shuttles substances through the lymph node but represents the morphological equivalent to the filtering function of the lymph node.

Introduction

Most primary adaptive immune responses are initiated in the T cell area of the lymph node. At this site, naive T cells, recirculating from the blood via HEVs, encounter DC that present processed peptides of previously acquired antigens in an MHC context (Banchereau and Steinman, 1998). Despite enormous progress in the field of DC biology and rapidly accumulating data on molecular mechanisms involved in the interplay between T cells and DC, relatively little is known about how these processes function in vivo within the complex structural environment of the intact lymphatic organ.

Upon microbial contact, DC within peripheral organs can phagocytose antigens and, subsequently, traffic via the afferent lymphatics into the T cell area of the draining lymph node to initiate immune responses (Cavanagh and Von Andrian, 2002; Manickasingham and Reis e Sousa, 2001; Randolph, 2001). This pathway is well characterized, and there is recent evidence that steady state migration of DC into the lymph node also occurs in the healthy organism, which may serve to continuously tolerize T cells against self antigens (Lutz and Schuler, 2002; Steinman et al., 2003). A second pathway of antigen delivery is less well defined and functions independently of cellular trafficking along the lymphatics. Several studies have shown that peripherally applied soluble antigen is taken up, presented, and cross presented by resident DC in the T cell area of the draining lymph node. This happens before there is any detectable immigration of DC from the periphery (Ingulli et al., 2002; Itano et al., 2003; Maurer et al., 2002; Pior et al., 1999). These pathways of antigen delivery result in two temporally distinct "waves" of antigen presentation within the lymph node, which have been shown to induce functionally different T cell responses (Itano and Jenkins, 2003). However, to date, the physical means of transport of the soluble antigen from the injection site to the DC has not been identified, although it was speculated as early as 1964 that the reticular fiber network of the lymph node may play a central role in this process (Moe, 1964).

The reticular network is a three-dimensional frame of collagen fibers that is closely ensheathed by the nonhematopoietic, fibroblastic reticular cells (FRC), resulting in a scaffold that physically connects the subcapsular and paracortical sinuses with the walls of the blood vessels (Anderson and Anderson, 1975; Anderson and Shaw, 1993; Gretz et al., 1997; Sainte-Marie and Peng, 1986; Ushiki et al., 1995). The FRC are tightly interconnected, resulting in a compartment that is separate from the T and B cell microenvironments. The concept that this network can serve as a conduit system for the transport of fluid and soluble substances within the lymph node stems from early morphological studies (Anderson and Anderson, 1975; Sainte-Marie and Peng, 1986). In addition, recent studies by Shaw and coworkers (Gretz et al., 2000) have shown that the conduit system allows low molecular weight substances (below 70 kDa), carried within the afferent lymph, to move directly from the subcapsular sinus to the lumen of HEVs without percolating through the lymphocyte compartment.

The physiological significance of this conduit system was recently shown in two studies (Baekkevold et al., 2001; Palframan et al., 2001): the authors demonstrated that within minutes after subcutaneous injection, chemokines are presented on the lumen of HEVs where they can act to recruit leukocytes. The fast delivery of chemokines occurred via the conduit system and was interpreted as a "remote control" function that serves

*Correspondence: sixt@biochem.mpg.de

to project the chemokine profile of the inflamed periphery to HEVs in order to redirect leukocyte recirculation from the blood. A similar conduit system has been reported to exist in the spleen where it delivers low molecular weight substances from the blood to the white pulp (Nolte et al., 2003). The concept that the reticular network of the lymph node might also serve as an antigen delivery system to antigen-presenting cells within the T cell zone is supported by ultrastructural investigations by Hayakawa and coworkers (Hayakawa et al., 1988). These authors demonstrated that the surface of the reticular fibers is not entirely covered by FRC but rather that approximately 10% of the fiber surface is occupied by macrophages and interdigitating DC, resulting in close contact to molecules delivered within the conduits.

In this study, we use a combined morphological, immunological, and cell biological approach to investigate how soluble antigens reach DC located inside the T cell area. We employ advanced light microscopic technology to investigate the detailed morphology of the conduit system and to define the exact pathway of soluble molecules within the lymph node. The nature of the extracellular matrix of the reticular fibers is characterized, revealing a core of interstitial collagen bundles surrounded by molecular components of microfibrils that are, in turn, ensheathed by a unique basement membrane-type structure. A combination of in vivo location studies and in vitro assays demonstrate that DC associate with the reticular fibers via specific interactions with components of the basement membrane, permitting close contact with the contents of the conduit system and, thereby, efficient uptake of small molecular weight substances from the conduit system.

Results

The Route of Soluble Tracers within Lymph Nodes

After subcutaneous injection, 40 kDa FITC-DEX accumulated in the subcapsular, paracortical, and medullary sinuses of the draining lymph node (Figure 1A). FITC-DEX also highlighted the entire reticular network of the lymph node as revealed by costaining with the basement membrane component perlecan (Figure 1B). Accumulation of tracer was apparent in the wall and lumen of HEVs (Figure 1A, insert). 3D reconstruction of FITC-DEX surrounding an HEV was performed (Figure 1C) to visualize the tracer transport route: FITC-DEX-derived fluorescence highlighted tracer located in reticular structures (arrows) that are continuous with the HEV margins (stars). Comparable results were obtained with recombinant soluble green fluorescent protein and FITC-OVA as tracers (data not shown). Fluorescence appeared immediately after injection of the tracer and was detectable in the conduits for up to 30–60 min.

Architecture and Molecular Composition of Reticular Fibers

Paraffin sections of FITC-DEX-loaded lymph nodes were costained with a broad range of antibodies against extracellular matrix molecules, and 3D reconstructions of the staining patterns were performed to define the molecular components of the reticular fibers and their organization. Figure 2B shows an example of the data obtained and illustrates the conduit structure consisting of a collagen type I core surrounded by basement membrane molecules (listed in Figure 2G). This structure is, in turn, ensheathed by a layer of smooth muscle actin, desmin, and gp38-positive FRC (Figures 2E and 2F, summarized in Figure 2G). Soluble tracer was found exclusively on the luminal side of the basement membrane, but not directly associated with it, as shown in the FITC-DEX-perlecan double fluorescence image in Figure 2A. Identical results were obtained with stainings for all basement membrane components listed in Figure 2G.

The monoclonal antibody ER-TR7, which recognizes an undefined antigen that is considered to be specific for FRC (Van Vliet et al., 1986), marked an extracellular compartment located between the collagen I core and the basement membrane (Figures 2C and 2D). Costainings revealed that the microfibrillar components, fibrillin-1 and -2, were localized at the same site (summarized in Figure 2G), demonstrating the existence of a third extracellular matrix layer that bridges the collagen I core with the adjacent basement membrane. All extracellular matrix components showed a compact tube or fiber-like distribution, whereas the FRC-specific stainings were more variable in diameter and appeared to surround the extracellular matrix staining throughout the whole T cell zone (Figure 2F).

All basement membrane components were found to enclose the collagen I core of the conduit system, including laminins, nidogen, collagen IV, and the heparan sulfate proteoglycan, perlecan. Fibronectin, a component of the interstitial matrix that can be associated with basement membranes in development or disease, also colocalized with basement membrane molecules. Because laminins are the functionally active components of basement membranes and occur in fifteen structurally and functionally distinct isoforms (Li et al., 2003), their occurrence in the conduit was studied in detail with chain specific antibodies: laminin 10 ($\alpha5\beta1\gamma1$) and laminin 8 ($\alpha4\beta1\gamma1$) were found to be the predominant isoforms in the conduit. Other laminins, such as laminin 1 ($\alpha1\beta1\gamma1$) and laminin 2 ($\alpha2\beta1\gamma1$), were not detected (summarized in Figure 2G).

Resident DC Are Associated with the Reticular Fibers

Several studies have shown that soluble antigen can be presented by lymph node resident DC in the T cell area long before DC immigration from the periphery occurs (Itano et al., 2003). To investigate whether resident DC acquire soluble antigen via the conduits, we investigated the relationship of DC to reticular fibers in healthy C57Bl/6 mice. Staining with a pan-laminin antibody to mark reticular fibers and with the DC marker CD11c revealed that 60% of DC occurred in direct association with reticular fibers (Figures 3A, 3E, and 3F). Staining for CD11b, which defines the myeloid DC subset in the paracortex of the T cell area, showed an even more pronounced (80%) association with the reticular fibers of the paracortex (Figures 3B and 3F).

Costaining of CD11b and CD11c was performed and revealed that CD11b-positive cells in the T cell area are

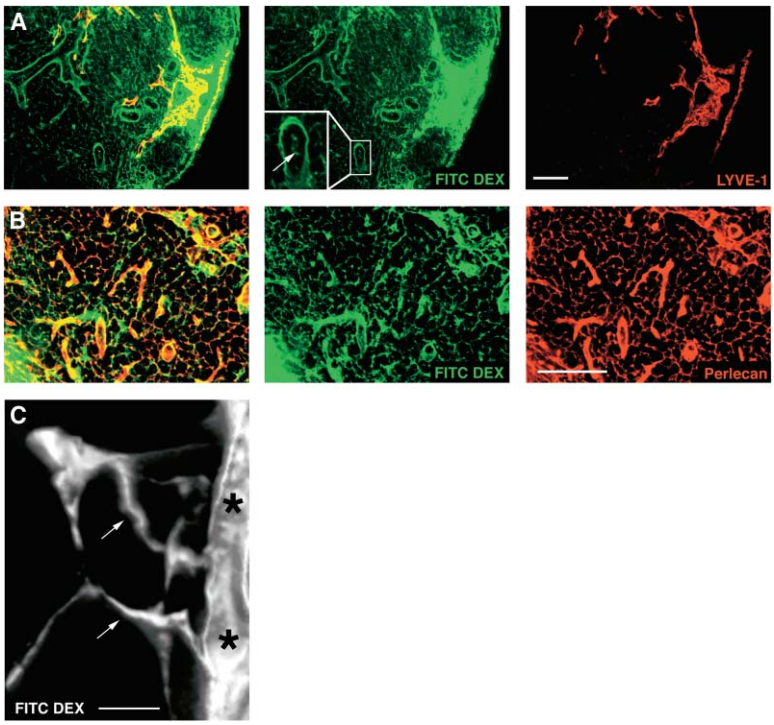

Figure 1. Localization of Tracer in Lymph Nodes

40 kDa lysine-fixable FITC-DEX was injected subcutaneously, and after one minute, the draining lymph node was excised and fixed with paraformaldehyde. Fixation prevents tracer from diffusing out of the section during washing steps. (A) Tracer accumulates mainly in the sinuses of draining lymph nodes, marked by LYVE-1 staining. Weaker tracer accumulation is present in a reticular pattern, surrounding HEVs and in the HEV lumen (insert). Size bar, 50 μm. (B) Tracer colocalizes with the basement membrane component, perlecan, in the reticular fibers of the T cell parenchyma. Size bar, 50 μm. (C) Three-dimensional reconstruction of tracer accumulating in an HEV wall (right margin of the picture). There is a continuous connection of the reticular fibers that are approaching from the left side (arrows) and the wall of the HEV (stars). Size bar, 10 μm.

also positive for CD11c and are, therefore, myeloid DC and not macrophages (Figure 3A). In contrast, nearly all CD11b-positive cells in the sinuses were CD11c negative and, therefore, macrophages (data not shown). This is in accordance with previous reports of the absence of macrophages in the T cell zone (Witmer and Steinman, 1984; Witmer-Pack et al., 1993). CD205-positive DC that localized mainly in the deep cortical area showed only 45% reticular fiber association (Figures 3F and 4B). Intense staining for β1 integrin at the contact zones between DC and reticular fibers (Figure 3E) suggested a role for cell-matrix interactions in the localization of resident DC to the reticular fibers.

The localization of mature DC that immigrated into the lymph node under inflammatory conditions was investigated: bone marrow-derived DC were stimulated overnight with lipopolysaccharide (LPS), CFSE labeled, and injected subcutaneously into the hind footpads of mice. 24 hr after injection, the labeled DC had migrated into the deep T cell areas of the draining popliteal lymph node and rarely associated with the reticular fibers (Figure 3C). Quantification revealed that only 19% of the CFSE-labeled DC showed overlapping staining with reticular fibers (Figure 3F). Similar results were obtained in a second series of experiments in which FITC-DEX together with LPS was injected into footpads, which triggers endogenous skin-derived DC to migrate into the draining lymph node after having taken up the tracer peripherally. 12–24 hr after injection, these DC were detected as bright FITC- and 2A1 (a marker for mature DC [Inaba et al., 1992])-positive cells in the T cell area without considerable association with the reticular fibers (Figures 3D and 3F). Taken together, lymph node resident DC during steady-state conditions show a direct interaction with the reticular fibers, whereas DC immigrating during inflammatory conditions show significantly less contact with reticular fibers.

Resident DC Are Able to Take Up and Process Soluble Antigen

The association of resident DC with reticular fibers is consistent with a role for the conduit system in the delivery of soluble antigens to resident DC. 40 kDa FITC-DEX was injected subcutaneously, and the draining lymph nodes were removed 90 min after injection to investigate this possibility. In contrast to the localization studies described above, methanol-fixed cryosections of lymph nodes were employed and stained for the DC markers, CD11c, CD11b, and CD205. Under these conditions, FITC-DEX diffuses out of the conduits during washing steps (Gretz et al., 2000) and remains exclusively in cells that have internalized it. FITC-DEX was found in CD11c- and CD11b-positive DC in the paracortical T cell areas, almost exclusively in association with the reticular fibers (Figures 3G and 3H). This finding strongly argues for DC antigen uptake via conduits. Also CD11b- and CD11c-negative cells close to the reticular fibers were found to accumulate FITC-DEX (not shown). These cells were negative for markers detecting FRC and lymphatic endothelial cells as well as CD3 and B220 (not shown) and remain to be identified. Furthermore, it was evident that not all CD11c- and CD11b-positive cells take up FITC-DEX despite close association with the reticular fibers, which might be due to the detection limits of light microscopy or to different phagocytic capabilities of the DC.

To investigate whether resident DC are capable of processing the acquired antigen, we utilized DQ-OVA as a tracer molecule. DQ-OVA is heavily labeled with fluorochrome, which results in an autoquenching effect

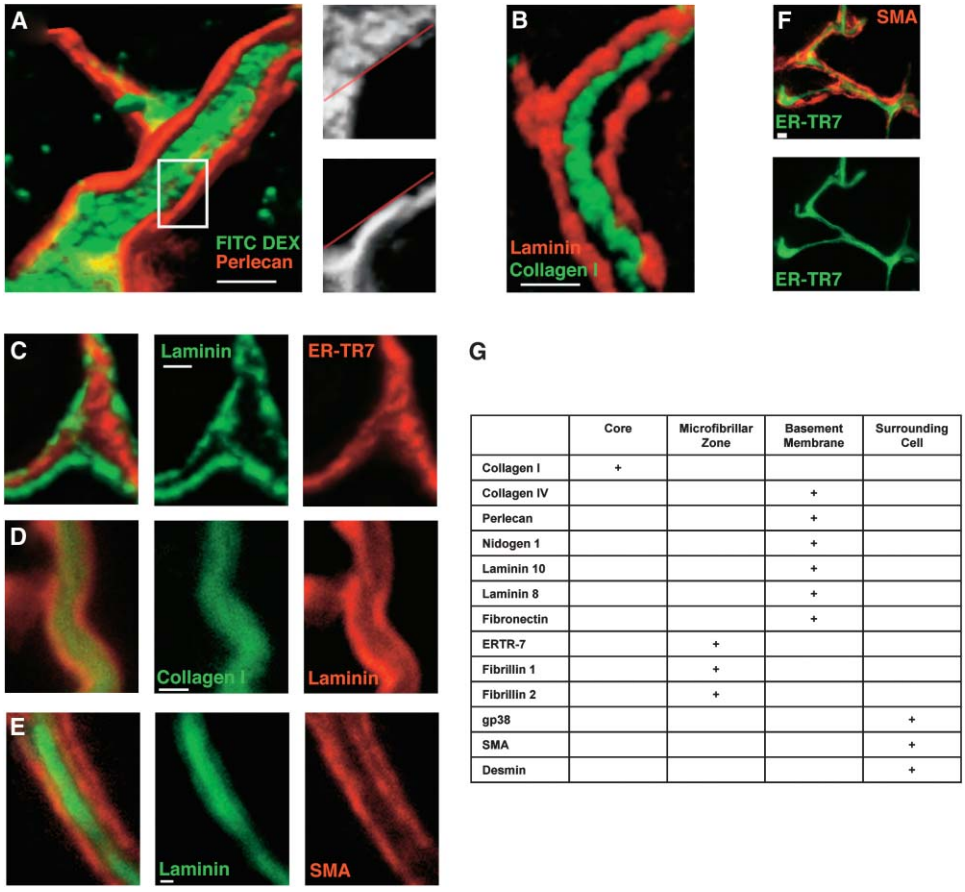

G

	Core	Microfibrillar Zone	Basement Membrane	Surrounding Cell
Collagen I	+			
Collagen IV			+	
Perlecan			+	
Nidogen 1			+	
Laminin 10			+	
Laminin 8			+	
Fibronectin			+	
ERTR-7		+		
Fibrillin 1		+		
Fibrillin 2		+		
gp38				+
SMA				+
Desmin				+

Figure 2. The Molecular Composition of the Conduit

Immunohistology of reticular fibers of the lymph node. Size bars, 1 μm. (A) Three dimensional reconstruction of a reticular fiber after 40 kDa FITC-DEX injection and staining for the basement membrane protein, perlecan, revealing that the basement membrane (highlighted by perlecan staining) encloses the compartment containing the tracer. High magnification of the boxed area shows no overlap of tracer and the basement membrane. The red line represents the same position in both images. (B) Double staining for pan-laminin and collagen type I. (C and D) The ER-TR7 antigen is located on the luminal side of the basement membrane but surrounding the collagen I. (E) Smooth muscle actin (SMA)-positive reticular fibroblasts surround the basement membrane. (F) SMA costaining with ER-TR7. (G) Summary of expression pattern of matrix molecules and FRC markers in and around the conduit.

that makes it undetectable in its unprocessed form. After proteolytic digestion, i.e., upon ingestion by phagocytes, the quenching effect is lost, and the tracer emits fluorescence in the green spectrum at low concentrations and red fluorescence at high concentrations. 90 min after injection of DQ-OVA, a strong fluorescent signal was detected in subcapsular, paracortical, and medullary sinuses (Figures 4A and 4B). Immunostaining of these sections with LYVE-1 as a marker for lymphatic endothelial cells (Prevo et al., 2001) and with CD11b as a marker for macrophages in the sinus (see above) revealed uptake and processing of tracer by both cell types, which are the prevailing cell types in the sinus. However, labeling of the LYVE-1-positive cells was considerably more intense than that observed in macrophages (Figure 4C) in accordance with previous reports that injected microspheres accumulate predominantly in nonhematopoietic cells of the lymph node sinuses (Glazyrin et al., 1995). Macrophages and lymphatic endothelial cells had internalized the tracer as staining remained associated with the cells in methanol fixed tissue sections.

A much weaker fluorescent signal was apparent in the T cell area in cells associated with the reticular fibers (Figure 4D). Costaining with CD11b, which identifies DC in the T cell area (see above), showed that most of these cells were myeloid DC (Figure 4D) located in the outer cortical areas surrounding B cell follicles (Figure 4B). In contrast, CD205-positive DC were located in the deep cortical areas (Figure 4B), and DQ-OVA-derived fluorescence of these DC was either absent or below the detection level. Taken together, DC located close to the conduits are able to process antigen taken up via the soluble route.

Immature DC Adhere and Are Immobile on Basement Membrane Components of the Conduits, whereas Mature DC Are Highly Motile and Nonadherent

The conduit basement membrane is immediately adjacent to the resident DC associated with the reticular fibers and may, therefore, act as an adhesive substrate holding DC at this site. In vitro adhesion and migration assays were performed with bone marrow-derived immature and mature DC and conduit extracellular matrix

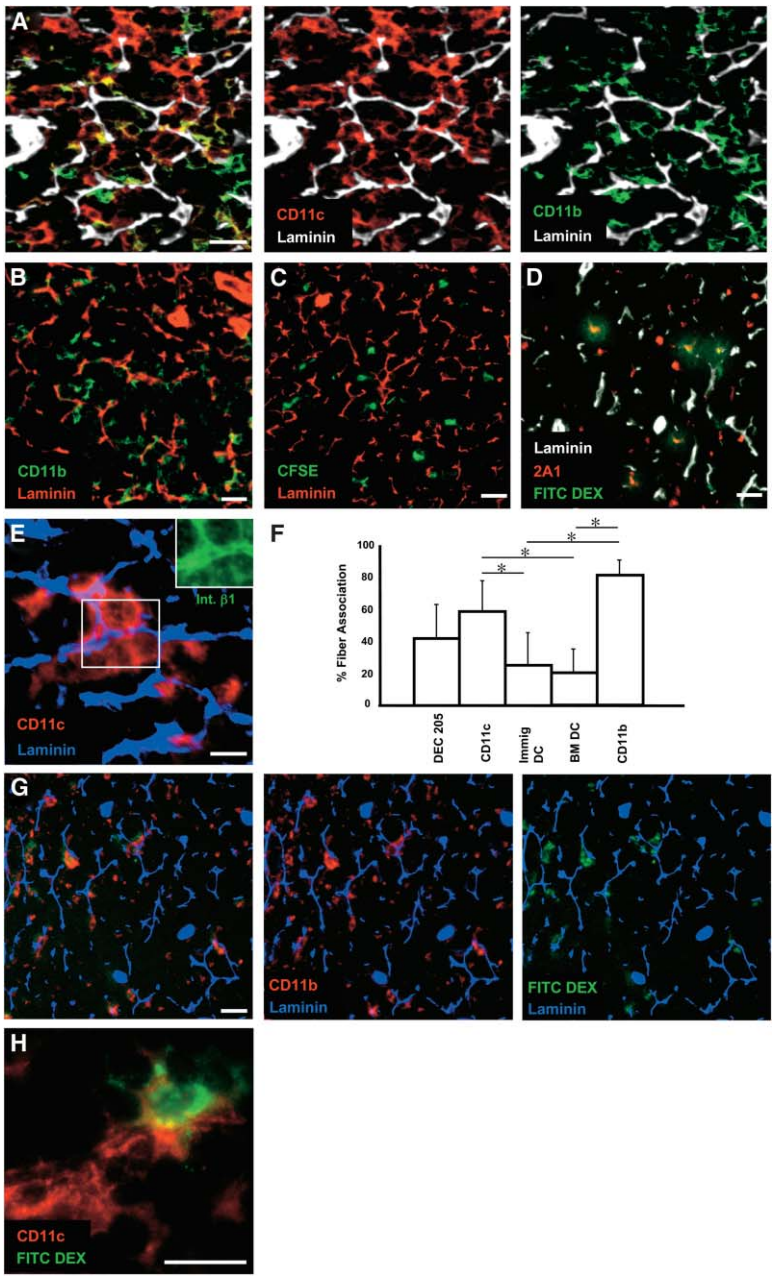

Figure 3. Association of Resident DC with the Reticular Fibers and Uptake of Tracer by Fiber-Associated DC

(A) Triple staining of CD11b, CD11c, and pan-laminin in the T cell area. Size bar, 20 μm.

(B) CD11b-positive resident DC and reticular fibers in the paracortical T cell zone.

(C) CFSE-labeled bone marrow-derived DC (green) 24 hr after subcutaneous injection immigrated into the lymph node and occurred remote from the fibers marked by pan-laminin staining.

(D) 24 hr after subcutaneous injection of 500 kDa FITC-DEX together with LPS, endogenous DC took up tracer in the periphery and immigrated into the T cell area. These DC were strongly FITC positive and also positive for the mature DC marker 2A1. Reticular fibers are stained with pan-laminin. Size bars, 20 μm.

(E) High magnification of CD11c-positive DC in the T cell area in close association with reticular fibers. The insert shows β1 integrin on the DC at the contact points with the reticular fiber. Size bar, 10 μm.

(F) Quantification of different DC subtypes and their association with reticular fibers. Values are the percentage of stainings of the indicated DC markers that overlap with pan-laminin staining. "BM-DC" represents the treatment in C, and "immig. DC" represents the treatment in D. Error bars represent the mean ± SD. Stars indicate $p < 0.05$ by T test.

(G) 90 min after subcutaneous injection 40 kDa FITC-DEX accumulates within CD11b-positive cells located near the fibers. Size bar, 20 μm.

(H) At higher magnification, FITC-DEX within a CD11c-positive cell. Size bar, 10 μm.

components as substrates to examine the possibility of adhesive interactions with conduit components. Substrates tested included collagen type I as representative of the core of the conduit and the conduit basement membrane-associated molecules, laminins 8 and 10, collagen type IV, perlecan, and fibronectin. Comparisons were made with basement membrane components that do not occur in the conduit system, including laminins 1 and 2 (Figure 5A). The only detectable binding was observed with immature DC on purified laminin 10 and fibronectin: 75% of the DC bound to fibronectin, and 92% bound to laminin 10 (Figures 5A and 5B). Binding to both substrates was of high affinity, which is in accordance with their occurrence in the conduit basement membrane. The specificity of the interaction between immature DC and laminin 10 is further supported by the fact that the other laminin isoforms tested were either not adhesive (laminins 8 and 2) or even repulsive in the case of laminin 1 (Figure 5B). In contrast to immature DC, terminally mature DC did not show significant binding to any of the extracellular matrix molecules tested (Figure 5B and data not shown). Similar but more variable results were obtained with DC isolated from lymph nodes as these DC start to undergo maturation during the isolation procedure (data not shown). Consistent with the polarized localization of β1 integrins at the contact points between immature DC and reticular fibers, the in vitro binding of immature DC to laminin 10 and fibronectin was abolished in the presence of a β1 integrin function-blocking antibody, Ha2/5, but not an isotype-matched control antibody (Figure 5C).

Two different techniques were employed to evaluate

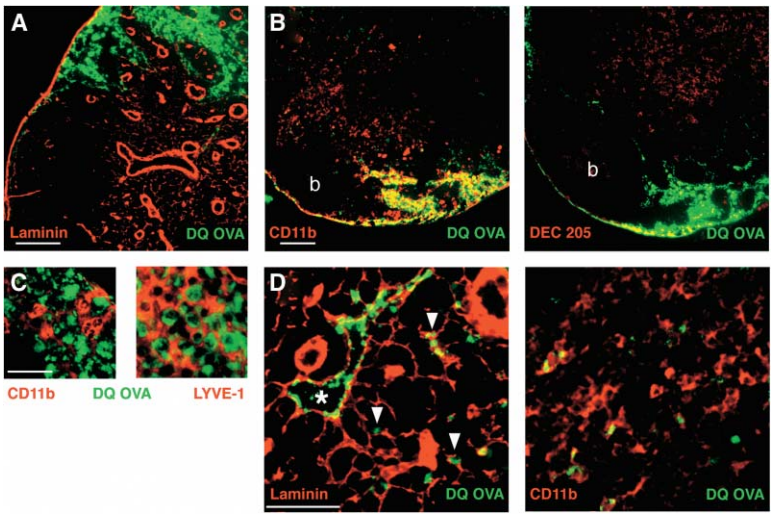

Figure 4. Processing of Soluble DQ-OVA in the Lymph Node

(A) 90 min after subcutaneous injection of 50 μg DQ-OVA, fluorescence is detected in the sinus area of the lymph node. Tissue was not paraformaldehyde-fixed, and, therefore, only ingested material is visualized. Size bars, 50 μm.

(B) Costaining with CD11b and DEC 205 on consecutive sections shows that the two DC subsets of the T cell area are located in the outer and deep cortex respectively and that DQ-OVA fluorescence is spatially associated with CD11b-positive cells. The bright fluorescent area at the bottom of the lymph node is a sinus. "b", B cell follicle.

(C) High magnification of a sinus area shows CD11b-positive macrophages to contain less DQ-OVA-derived fluorescence compared to LYVE-1-positive sinus cells. Size bars, 10 μm.

(D) Left: high magnification of an outer cortical area shows DQ-OVA-derived fluorescence associated with reticular fibers of the T cell area. The star marks a sinus, and arrowheads mark DQ-OVA-containing cells attached to conduits. Right: DQ-OVA-positive cells in the T cell area are mainly CD11b positive. Size bar, 50 μm.

random DC migration on extracellular matrix substrates, revealing a negative correlation between strength of adhesion and motility. In general, immature DC showed less random migration in a transwell system than mature DC (Figures 6A and 6B). However, random migration of immature DC was significantly reduced on laminin 10 and fibronectin. In contrast, mature DC showed high levels of random motility regardless of the substrate coated (Figure 6B). Similar results were obtained when motility was analyzed by time lapse video microscopy of DC randomly migrating on extracellular matrix coated on two-dimensional surfaces. On laminin 10 and fibronectin, immature DC showed a spread and immobilized phenotype, whereas mature DC were dendritic and highly motile regardless of the substrate (see Supplemental Movies 1 and 2 available online at http://www.immunity.com/cgi/content/full/22/1/19/DC1/).

Discussion

It has been shown that antigen presentation to T cells after subcutaneous application of soluble antigen occurs in two "waves": first, lymph node resident DC take up and subsequently present antigen, a process that is initiated within minutes after antigen application. Only much later, after 8–12 hr, immigrated DC that have acquired antigen at the injection site arrive in the T cell zone (Itano and Jenkins, 2003; Itano et al., 2003). The data presented here elucidate the cellular and extracellular microanatomy of the reticular fiber network and demonstrate how these features serve to form the infrastructure that is essential for the first wave of antigen presentation.

Soluble tracers applied peripherally are transported with the interstitial fluid along the lymphatic vessels into the sinus areas of the draining lymph node. We show here that the reticular cells of the sinuses as well as the sinus lining cells show molecular characteristics of lymphatic endothelial cells and share their high capacity to take up soluble molecules. They phagocytose and process tracer with greater efficiency than the sinusoidal macrophages. Soluble antigens in the subcapsular sinuses can then take two further routes that are determined by their size. Shaw and coworkers (Gretz et al., 2000) have shown that molecules over 70 kDa circumvent the lymphocyte compartment and are drained along the sinuses into the efferent lymph vessel. Molecules smaller than 70–80 kDa are transported through the enclosed compartment of the reticular network known as the conduit system into the lumen of the HEV. Our data demonstrate that the conduit system of the reticular network is a highly specialized extracellular matrix consisting of a central core formed by interstitial matrix molecules, such as collagen type I as shown here and collagen type III (Kaldjian et al., 2001; Karttunen et al., 1989), that is surrounded by a basement membrane-like structure and, in turn, ensheathed by a layer of FRC. The basement membrane of the conduit is unique, because it does not separate two cellular compartments as basement membranes usually do but, rather, surrounds an acellular lumen consisting of a highly specialized interstitial matrix. Tracer is transported on the luminal side of the basement membrane, and it is, therefore, noteworthy that the molecular composition of the conduit basement membrane is similar to that underlying endothelial cells. It contains the endothelial cell laminin isoforms, laminins 8 and 10, which have been shown to contribute to the barrier function of vascular endothelium (Sixt et al., 2001a; Thyboll et al., 2002).

An additional extracellular matrix layer containing fibrillin-1 and fibrillin-2 exists between the collagen core and the basement membrane. Fibrillins constitute the structural backbone of supramolecular fibrillar aggregates, 10–12 nm in diameter, called microfibrils (Sakai et al., 1986; Zhang et al., 1994). This observation is consistent with ultrastructural studies that have shown bundles of microfibrils surrounding the collagen core of the reticular fiber (Hayakawa et al., 1990). Microfibrils are found in many elastic and nonelastic tissues where they fulfill diverse functions. For example, microfibrils in the ciliary zonule of the eye transmit forces for visual accom-

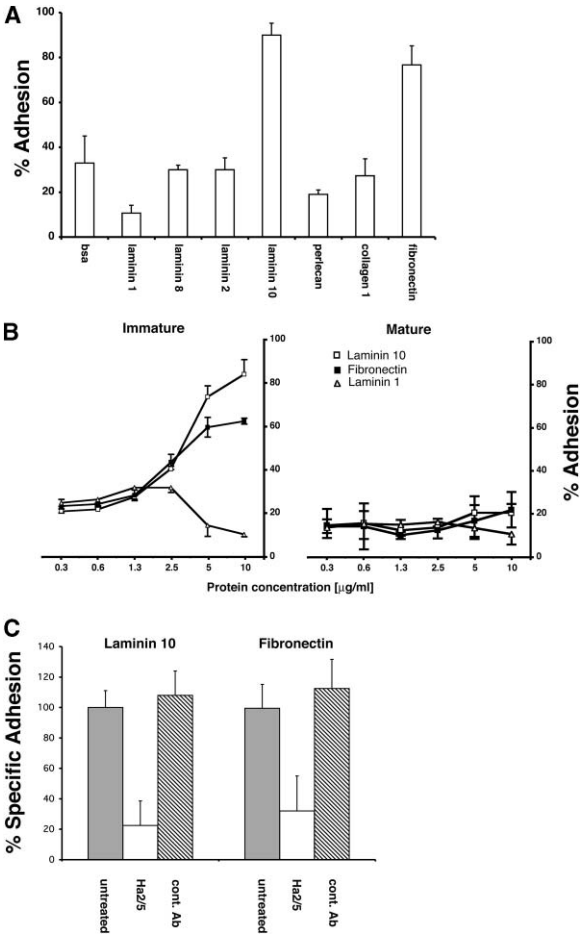

Figure 5. Adhesion of Bone Marrow-Derived DC to Purified Extracellular Matrix Molecules

(A) Immature DC binding to the conduit basement membrane components, fibronectin and laminin 10, and to other nonconduit extracellular matrix molecules (laminin 1 and 2) or to collagen type I, a component of the conduit core.

(B) Adhesion of immature and mature DC to laminin 10 and fibronectin coated at different concentrations.

(C) Adhesion of immature DC to laminin 1 and 10 and fibronectin in the presence of 10 μg/ml of the function-blocking β1 integrin antibody, Ha2/5, and in the presence of an isotype-matched control antibody. Untreated denotes binding in the absence of added antibody. Each experiment was performed three times, and values represent means of triplicates ± SD of one representative experiment.

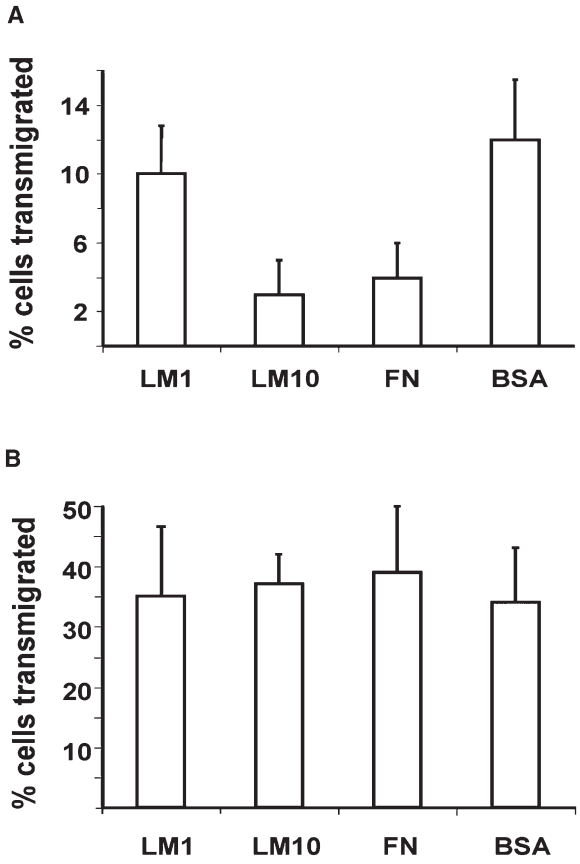

Figure 6. Random Transmigration of Immature and Mature DC

Migration of immature (A) and mature (B) bone marrow-derived DC across transwell filters (8 μm pore size) coated with 5 μg/ml laminin 1 (LM1) or 10 (LM10) or fibronectin (FN). 5×10^4 cells were added per filter and allowed to transmigrate for 2.5 hr at 37°C; the total number of cells was counted in the lower chamber, and the percentage of transmigrated cells was calculated. Values represent means of at least four separate experiments ± SD.

modation, and microfibrils in the aortic wall have a role in vascular homeostasis (Pereira et al., 1997). In the conduits, it is likely that the microfibrils not only fill the space between the basement membrane and the collagen core but physically connect these structures. There are many examples where microfibrils intersect basement membranes such as in lung, kidney, skin, and other tissues. It is further possible that this microfibrillar meshwork represents the filtering unit of the conduit or contributes to its stability and elastic properties.

The conduit, as a shortcut from the sinus to the HEV, is of physiological importance for the transport of chemokines that are produced in peripheral inflamed tissues but act at the level of the HEV lumen to control lymphocyte recruitment (Baekkevold et al., 2001; Palframan et al., 2001). However, the concept of a sealed conduit system that opens only into the HEV lumen does not explain how soluble antigens drained from the interstitial fluid can be acquired by lymph node resident DC. A selective filtering function of the lymph node requires some possibility for substance exchange between the conduit compartment and that of the surrounding hematopoietic cells. We show that the strategic position of resident DC along the conduits enables them to take up soluble antigen (see Figure 7). Using the fluorescent properties of DQ-OVA, we were able to show that these DC can also process the acquired antigen. This is consistent with previously published flow cytometric analyses of lymph node resident DC after subcutaneous tracer injection, which showed that resident DC take up and present soluble molecules to T cells (Ingulli et al., 2002; Itano et al., 2003). We further show that mature DC that immigrated into the lymph node from the periphery during inflammatory conditions were not attached to the conduits and occurred between the T cells. This is in accordance with their physiological function, because mature DC have already acquired antigen in the periphery and do not require access to substances arriving

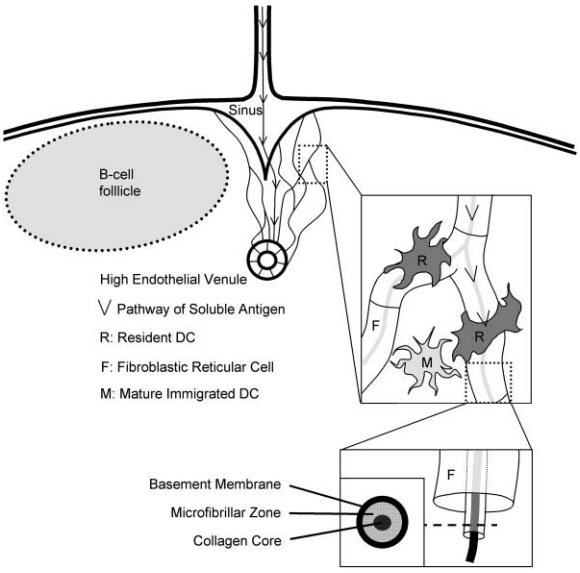

Figure 7. Schematic Representation of the Conduit Architecture and the Pathway of Soluble Molecules inside the Lymph Node

Soluble molecules enter the sinus areas via the afferent lymphatic vessels from where the low molecular weight fraction enters the conduit system and is drained into the HEV. The conduits are mainly covered with FRC, but also resident DC have contact with the basement membrane that constitutes the wall of the conduit. Because of this close proximity, resident DC are able to contact and take up antigens that are filtered through the lymph node. Terminally mature DC that have immigrated from the periphery during inflammatory states do not associate with conduits and, therefore, do not have access to their contents.

with the interstitial fluid. The observation that resident DC are in close contact with the conduits and have access to their contents extends the function of the conduits as an "information highway": soluble molecules can not only be delivered from the periphery to the lumen of HEV and "remote control" leukocyte recirculation. Also, resident DC can be rapidly informed about the state of the periphery via this pathway.

The difference in localization of resident immature DC and immigrating mature DC correlates well with the ability of in vitro-generated DC to bind and migrate on the extracellular matrix components of the reticular fiber. Only the conduit basement membrane components, fibronectin and laminin 10, supported adhesion of immature DC, whereas no binding or even repulsion was observed on extracellular matrix molecules that occur in the core of the conduit or do not occur in conduits. Consistent with the in vivo location of β1 integrins at the interface between immature DC and the reticular fiber surface, the adhesion to both fibronectin and laminin 10 was mainly mediated by β1 integrins. The adhesive and migratory capacity of in vitro-generated DC changed dramatically upon maturation: immature DC showed reduced motility on the adhesive conduit basement membrane components. Upon maturation, DC became highly motile regardless of the extracellular matrix molecules that they encountered. This difference was not due to a downregulation of surface integrins (M. Sixt, unpublished data) but, rather, to a functional inactivation of the receptors upon DC maturation. In mature DC, integrins were inactive and only upon chemokine triggering were they transiently activated (M. Sixt, submitted). These adhesive and migratory properties seem to be a general feature of immature versus mature DC that are reflected by in vitro-generated DC. In vivo, different DC subsets might have different abilities to localize to conduits as has been suggested recently (Pribila et al., 2004a, 2004b). However, care has to be taken when assaying the cell biology of DC freshly isolated from lymph nodes as isolation procedures always trigger maturation and, therefore, do not allow investigation of resident DC in their natural maturation state.

Taken together, our results suggest that the conduit basement membrane serves as a specific anchoring structure for resident DC resulting in close contact between the DC and the conduit contents. The ability to interact with the conduit basement membrane is lost upon DC maturation, thereby permitting the mature DC to become highly motile and to move freely in the T cell compartment to maximize T cell-DC encounters.

Apart from their significance for the transport of soluble antigens within the lymph node, the data we present here have general implications to studies of lymphocyte trafficking inside secondary lymphoid organs. We show that none of the investigated extracellular matrix molecules are directly exposed to the lymphocyte compartment but rather that the extracellular matrix is covered by the layer of FRC and the occasional resident DC. Hence, within the lymph node collagens, fibronectin and laminins are not exposed to lymphocytes, which makes it unlikely that the direct costimulatory effects of these molecules that have been reported in several studies are of physiological relevance within the intact lymph node.

Experimental Procedures

Animals

All animal experiments were performed with C57Bl/6 mice of 4–10 weeks of age obtained from the breeding facility of the Institute of Experimental Pathology, Lund, Sweden. Animals were kept under pathogen-free conditions and according to animal ethics regulations.

Reagents

Tracers

40 and 500 kDa lysin-fixable FITC-Dextran (DEX), DQ-Ovalbumin (OVA), and FITC-OVA were obtained from Molecular Probes (Leiden, Netherlands) and diluted to 5 mg/ml in phosphate buffered saline (PBS). DQ-OVA is an autoquenched conjugate of OVA and the fluorescent label BODIPY. Only upon proteolytic digestion can the fluorochrome be excited to emit in the green spectrum. At high concentrations, as occurs in phagocytotic compartments, BODIPY forms excimers emitting in the red spectrum.

Antibodies

Antibodies employed to extracellular molecules recognized three major extracellular matrix types, basement membranes, interstitial matrices, or microfibrils. Cellular markers employed are listed below.

Basement Membrane

Rat anti-mouse laminin γ1 (3E10) (Sixt et al., 2001a), rat anti-mouse laminin α2 (4H8-2) (Schuler and Sorokin, 1995), rat anti-mouse laminin β1 (3A4) (Sixt et al., 2001b), rabbit anti-mouse laminin 1 (247) (Sorokin et al., 1990), rabbit anti-mouse perlecan (Klein et al., 1995), rabbit anti-mouse nidogen-1 (Fox et al., 1991), rabbit anti-mouse laminin α4 (377) (Ringelmann et al., 1999), rabbit anti-mouse laminin α5 (405) (Ringelmann et al., 1999), rabbit anti-mouse collagen IV (Chemicon, Hofheim, Germany), and rabbit anti-mouse fibronectin (GIBCO, Germany).

Interstitial Matrix Molecules and Microfibrils

Rabbit anti-mouse collagen 1 (Chemicon), rabbit anti-human fibrillin-1 and rabbit anti-human fibrillin-2 (both anti-human fibrillin antisera cross react with mouse fibrillin-1 and -2 [Lin et al., 2002]), and rat anti-mouse ER-TR7 (Van Vliet et al., 1986).

Cellular Markers

Hamster anti-mouse β1 integrin (Ha2/5) (Pharmingen, Heidelberg, Germany), rabbit anti-mouse β1 integrin (Bottger et al., 1989), cy3-coupled mouse anti-smooth muscle actin (Sigma Aldrich, Stockholm, Sweden), hamster anti-mouse CD11c (N418) (ATCC), rat anti-mouse CD11b (M1/70) (ATCC), rat anti-mouse 2A1 (Inaba et al., 1992), rat anti-mouse CD205 (DEC 205, NLDC145) (ATCC), and hamster anti-mouse gp38 clone 8.1.1 (Farr et al., 1992). A rat anti-mouse LYVE-1 antibody was produced with the entire extracellular domain of LYVE-1, as previously described for generation of a rabbit polyclonal serum, and showed the same staining patterns as the previously reported antibody (Prevo et al., 2001).

Injection of Soluble Tracers or Cells and Animal Preparation

Tracers were injected subcutaneously into hind footpads in 20 μl PBS. Mice were sacrificed immediately (approximately 1 min) after injection or at the indicated time points by CO_2 asphyxiation. For DC localization studies, mature DC were labeled with 5 μM 5,6-carboxyfluorescein diacetate succiniminidyl ester (CFSE) for 8 min according to the manufacturer's recommendations (Molecular Probes). After labeling, 5×10^5 DC in a volume of 30 μl were injected into the hind footpads. 50 μg 500 kDa FITC-DEX was injected together with 5 μg LPS (Sigma-Aldrich; *E. coli*, 0127:B8) into footpads to track the migration of endogenous DC.

Immunofluorescence

Cryostat sections (6–8 μm) were fixed and blocked as described previously (Sixt et al., 2001a), and bound antibodies (if not directly labeled) were visualized with FITC-, cy3-, or cy5-conjugated goat anti-rat and goat anti-rabbit IgG secondary antibodies (Dianova, Hamburg, Germany) and Alexa Fluor 594-conjugated goat anti-hamster antibody (Molecular Probes). Paraformaldehyde-fixed sections were embedded in paraffin and processed by standard protocols. Sections of 8–10 μm were cut and incubated with 1 mg/ml Pronase (Sigma) for 15 min at 37°C prior to staining. Stained sections were examined with either a Zeiss Axiophot or Axiovert 200M fluorescence microscope and documented with a Hamamatsu ORCA1 camera and the Openlab software (version 3.1.2; Improvision, London, UK). Three-dimensional reconstructions were generated by performing z scans and subsequent image deconvolution and reconstruction with Improvision Velocity 2.5 software.

Quantification of Immunofluorescence:

A cell was considered to be in contact with a fiber if its staining showed overlap with the pan-laminin immunofluorescence. Each value was obtained from six different lymph nodes collected from six different animals, and the relative location of 100 cells was determined in 2–5 sections per lymph node. T test was performed with Sigma Stat.

Adhesion Assays

In vitro cell attachment assays were performed as described previously (Sixt et al., 2001b) with the following purified extracellular matrix molecules as substrates: mouse laminin 1, mouse perlecan, and mouse collagen IV isolated from Engelbreth Holm Swarm Tumor (Paulsson et al., 1987), laminin 2 purified from mouse hearts (Paulsson and Saladin, 1989), laminin 8 purified from conditioned media of the Mc3T3-G2/PA6 preadipocyte cell line (Sixt et al., 2001b), laminin 10 isolated from human placenta, rat tail collagen 1 from Roche Diagnostics Corporation (Penzberg, Germany), human fibronectin isolated from plasma by gelatin-Sepharose chromatography (Vuento and Vaheri, 1979).

Bone marrow-derived DC at day 8 of culture were washed with PBS, and 5×10^4 cells were added per well in 100 μl adhesion buffer (RPMI, 0.5% BSA, 10 mM HEPES [pH7.5]). The number of adherent cells after 30 min incubation at 37°C without shear stress was determined by colorimetric analysis of lysosomal hexoaminidase (Sigma) (Landegren, 1984).

Antibody inhibition studies were carried out with hamster anti-mouse integrin β1 antibody Ha2/5 (Pharmingen). Cells were preincubated with the blocking or control antibody for 30 min at 37°C and, subsequently, added to the microtiter plates coated with 10 μg/ml of extracellular matrix proteins (Sixt et al., 2001b). The percentage of cells that bound specifically to the coated substrate was determined as follows: ((OD 405 total bound cells − OD 405 bound cells)/OD 405 of 50,000 cells applied) × 100 = percentage of specific binding.

Transwell Migration Assay

Filters of transwell chambers with 8 μm pore size (Costar, Bodenheim, Germany) were coated with the different matrix proteins at a concentration of 5 μg/ml, and membranes were subsequently blocked with 1% bovine serum albumin (BSA) fraction V (Sigma) and 50,000 cells were placed in the upper chamber of each well. After 2.5 hr at 37°C, cells on the bottom of the lower chamber were collected by washing with 5 mM EDTA and counted manually.

Time Lapse Video Microscopy

5 μl aliquots of extracellular matrix molecules (concentration of 5 μg/ml) were dotted onto superfrost plus slides (Menzel, Braunschweig, Germany), and proteins were allowed to bind at 37°C for 30 min. Slides were subsequently blocked with 1% BSA in PBS and placed in culture dishes. DC were added, and the interface between extracellular matrix coated and noncoated areas was observed by time lapse video microscopy. Experiments were performed at 37°C and 5% CO_2 in a humidified chamber, and images were collected at 30 s intervals with a Zeiss Axiovert 200M microscope controlled by Openlab software.

Generation of Bone Marrow-Derived DC

DC were generated from bone marrow cells derived from C57BL/6 mice according to a standard protocol (Lutz et al., 1999). Immature DC were pulsed overnight with either 500 U/ml TNF (Pepro Tech, Rocky Hill, New Jersey) or 1 μg/ml LPS (Sigma-Aldrich; *E. coli*, 0127:B8) on days 9–11 of culture to induce DC maturation.

Acknowledgments

M.S. was supported by fellowships from the European Union (Marie Curie fellowship, MEIF-CT-2003-501289), Anna-Greta Crafoord Foundation for Rheumatological Research, and Novartis. The work was further supported by grants from Fysiografisca Society and Oesterlund Stiftelse to L.S. and M.S. and from Knut och Alice Wallenberg Stiftelse (grant KAW 2002.0056) and the Swedish Medical Council (grant 621-2001-2141 to L.S.). N.K. was supported by the Uehara Memorial Foundation.

Received: December 11, 2003
Revised: November 4, 2004
Accepted: November 10, 2004
Published: January 25, 2005

References

Anderson, A.O., and Anderson, N.D. (1975). Studies on the structure and permeability of the microvasculature in normal rat lymph nodes. Am. J. Pathol. *80*, 387–418.

Anderson, A.O., and Shaw, S. (1993). T cell adhesion to endothelium: the FRC conduit system and other anatomic and molecular features which facilitate the adhesion cascade in lymph node. Semin. Immunol. *5*, 271–282.

Baekkevold, E.S., Yamanaka, T., Palframan, R.T., Carlsen, H.S., Reinholt, F.P., von Andrian, U.H., Brandtzaeg, P., and Haraldsen, G. (2001). The CCR7 ligand elc (CCL19) is transcytosed in high endothelial venules and mediates T cell recruitment. J. Exp. Med. *193*, 1105–1112.

Banchereau, J., and Steinman, R.M. (1998). Dendritic cells and the control of immunity. Nature *392*, 245–252.

Bottger, B.A., Hedin, U., Johansson, S., and Thyberg, J. (1989). Integrin-type fibronectin receptors of rat arterial smooth muscle cells: isolation, partial characterization and role in cytoskeletal orga-

nization and control of differentiated properties. Differentiation *41*, 158–167.

Cavanagh, L.L., and Von Andrian, U.H. (2002). Travellers in many guises: the origins and destinations of dendritic cells. Immunol. Cell Biol. *80*, 448–462.

Farr, A.G., Berry, M.L., Kim, A., Nelson, A.J., Welch, M.P., and Aruffo, A. (1992). Characterization and cloning of a novel glycoprotein expressed by stromal cells in T-dependent areas of peripheral lymphoid tissues. J. Exp. Med. *176*, 1477–1482.

Fox, J.W., Mayer, U., Nischt, R., Aumailley, M., Reinhardt, D., Wiedemann, H., Mann, K., Timpl, R., Krieg, T., Engel, J., et al. (1991). Recombinant nidogen consists of three globular domains and mediates binding of laminin to collagen type IV. EMBO J. *10*, 3137–3146.

Glazyrin, A.L., Kolesnikov, S.I., Dragun, G.N., Zelentsov, E.L., Zolotarev, K.V., Zorin Yu, A., Kulipanov, G.N., Gorchakov, V.N., and Dolbnya, I.P. (1995). Distribution of colloidal gold tracer within rat parasternal lymph nodes after intrapleural injection. Anat. Rec. *241*, 175–180.

Gretz, J.E., Anderson, A.O., and Shaw, S. (1997). Cords, channels, corridors and conduits: critical architectural elements facilitating cell interactions in the lymph node cortex. Immunol. Rev. *156*, 11–24.

Gretz, J.E., Norbury, C.C., Anderson, A.O., Proudfoot, A.E., and Shaw, S. (2000). Lymph-borne chemokines and other low molecular weight molecules reach high endothelial venules via specialized conduits while a functional barrier limits access to the lymphocyte microenvironments in lymph node cortex. J. Exp. Med. *192*, 1425–1440.

Hayakawa, M., Kobayashi, M., and Hoshino, T. (1988). Direct contact between reticular fibers and migratory cells in the paracortex of mouse lymph nodes: a morphological and quantitative study. Arch. Histol. Cytol. *51*, 233–240.

Hayakawa, M., Kobayashi, M., and Hoshino, T. (1990). Microfibrils: a constitutive component of reticular fibers in the mouse lymph node. Cell Tissue Res. *262*, 199–201.

Inaba, K., Inaba, M., Romani, N., Aya, H., Deguchi, M., Ikehara, S., Muramatsu, S., and Steinman, R.M. (1992). Generation of large numbers of dendritic cells from mouse bone marrow cultures supplemented with granulocyte/macrophage stimulating factor. J. Exp. Med. *176*, 1693–1702.

Ingulli, E., Ulman, D.R., Lucido, M.M., and Jenkins, M.K. (2002). In situ analysis reveals physical interactions between CD11b+ dendritic cells and antigen-specific CD4 T cells after subcutaneous injection of antigen. J. Immunol. *169*, 2247–2252.

Itano, A.A., and Jenkins, M.K. (2003). Antigen presentation to naive CD4 T cells in the lymph node. Nat. Immunol. *4*, 733–739.

Itano, A.A., McSorley, S.J., Reinhardt, R.L., Ehst, B.D., Ingulli, E., Rudensky, A.Y., and Jenkins, M.K. (2003). Distinct dendritic cell populations sequentially present antigen to CD4 T cells and stimulate different aspects of cell-mediated immunity. Immunity *19*, 47–57.

Kaldjian, E.P., Gretz, J.E., Anderson, A.O., Shi, Y., and Shaw, S. (2001). Spatial and molecular organization of lymph node T cell cortex: a labyrinthine cavity bounded by an epithelium-like monolayer of fibroblastic reticular cells anchored to basement membrane-like extracellular matrix. Int. Immunol. *13*, 1243–1253.

Karttunen, T., Sormunen, R., Risteli, L., Risteli, J., and Autio-Harmainen, H. (1989). Immunoelectron microscopic localization of laminin, type IV collagen, and type III pN-collagen in reticular fibers of human lymph nodes. J. Histochem. Cytochem. *37*, 279–286.

Klein, G., Conzelmann, S., Beck, S., Timpl, R., and Muller, C.A. (1995). Perlecan in human bone marrow: a growth-factor-presenting, but anti-adhesive, extracellular matrix component for hematopoietic cells. Matrix Biol. *14*, 457–465.

Landegren, U. (1984). Measurement of cell numbers by means of the endogenous enzyme hexosaminidase. Applications to detection of lymphokines and cell surface antigens. J. Immunol. Methods *67*, 379–388.

Li, S., Edgar, D., Fassler, R., Wadsworth, W., and Yurchenco, P.D. (2003). The role of laminin in embryonic cell polarization and tissue organization. Dev. Cell *4*, 613–624.

Lin, G., Tiedemann, K., Vollbrandt, T., Peters, H., Batge, B., Brinckmann, J., and Reinhardt, D.P. (2002). Homo- and heterotypic fibrillin-1 and -2 interactions constitute the basis for the assembly of microfibrils. J. Biol. Chem. *277*, 50795–50804.

Lutz, M.B., and Schuler, G. (2002). Immature, semi-mature and fully mature dendritic cells: which signals induce tolerance or immunity? Trends Immunol. *23*, 445–449.

Lutz, M.B., Kukutsch, N., Ogilvie, A.L., Rossner, S., Koch, F., Romani, N., and Schuler, G. (1999). An advanced culture method for generating large quantities of highly pure dendritic cells from mouse bone marrow. J. Immunol. Methods *223*, 77–92.

Manickasingham, S.P., and Reis e Sousa, C. (2001). Mature T cell seeks antigen for meaningful relationship in lymph node. Immunology *102*, 381–386.

Maurer, T., Heit, A., Hochrein, H., Ampenberger, F., O'Keeffe, M., Bauer, S., Lipford, G.B., Vabulas, R.M., and Wagner, H. (2002). CpG-DNA aided cross-presentation of soluble antigens by dendritic cells. Eur. J. Immunol. *32*, 2356–2364.

Moe, R.E. (1964). Electron microscopic appearance of the parenchyma of lymph nodes. Am. J. Anat. *114*, 341–369.

Nolte, M.A., Belien, J.A., Schadee-Eestermans, I., Jansen, W., Unger, W.W., van Rooijen, N., Kraal, G., and Mebius, R.E. (2003). A conduit system distributes chemokines and small blood-borne molecules through the splenic white pulp. J. Exp. Med. *198*, 505–512.

Palframan, R.T., Jung, S., Cheng, G., Weninger, W., Luo, Y., Dorf, M., Littman, D.R., Rollins, B.J., Zweerink, H., Rot, A., and von Andrian, U.H. (2001). Inflammatory chemokine transport and presentation in HEV: a remote control mechanism for monocyte recruitment to lymph nodes in inflamed tissues. J. Exp. Med. *194*, 1361–1373.

Paulsson, M., and Saladin, K. (1989). Mouse heart laminin. Purification of the native protein and structural comparison with Engelbreth-Holm-Swarm tumor laminin. J. Biol. Chem. *264*, 18726–18732.

Paulsson, M., Aumailley, M., Deutzmann, R., Timpl, R., Beck, K., and Engel, J. (1987). Laminin-nidogen complex. Extraction with chelating agents and structural characterization. Eur. J. Biochem. *166*, 11–19.

Pereira, L., Andrikopoulos, K., Tian, J., Lee, S.Y., Keene, D.R., Ono, R., Reinhardt, D.P., Sakai, L.Y., Biery, N.J., Bunton, T., et al. (1997). Targetting of the gene encoding fibrillin-1 recapitulates the vascular aspect of Marfan syndrome. Nat. Genet. *17*, 218–222.

Pior, J., Vogl, T., Sorg, C., and MacHer, E. (1999). Free hapten molecules are dispersed by way of the bloodstream during contact sensitization to fluorescein isothiocyanate. J. Invest. Dermatol. *113*, 888–893.

Prevo, R., Banerji, S., Ferguson, D.J., Clasper, S., and Jackson, D.G. (2001). Mouse LYVE-1 is an endocytic receptor for hyaluronan in lymphatic endothelium. J. Biol. Chem. *276*, 19420–19430.

Pribila, J.T., Itano, A.A., Mueller, K.L., and Shimizu, Y. (2004a). The alpha 1 beta 1 and alpha E beta 7 integrins define a subset of dendritic cells in peripheral lymph nodes with unique adhesive and antigen uptake properties. J. Immunol. *172*, 282–291.

Pribila, J.T., Quale, A.C., Mueller, K.L., and Shimizu, Y. (2004b). Integrins and T cell-mediated immunity. Annu. Rev. Immunol. *22*, 157–180.

Randolph, G.J. (2001). Dendritic cell migration to lymph nodes: cytokines, chemokines, and lipid mediators. Semin. Immunol. *13*, 267–274.

Ringelmann, B., Roder, C., Hallmann, R., Maley, M., Davies, M., Grounds, M., and Sorokin, L. (1999). Expression of laminin alpha1, alpha2, alpha4, and alpha5 chains, fibronectin, and tenascin-C in skeletal muscle of dystrophic 129ReJ dy/dy mice. Exp. Cell Res. *246*, 165–182.

Sainte-Marie, G., and Peng, F.S. (1986). Diffusion of a lymph-carried antigen in the fiber network of the lymph node of the rat. Cell Tissue Res. *245*, 481–486.

Sakai, L.Y., Keene, D.R., and Engvall, E. (1986). Fibrillin, a new 350-kD glycoprotein, is a component of extracellular microfibrils. J. Cell Biol. *103*, 2499–2509.

Schuler, F., and Sorokin, L.M. (1995). Expression of laminin isoforms in mouse myogenic cells in vitro and in vivo. J. Cell Sci. *108*, 3795–3805.

Sixt, M., Engelhardt, B., Pausch, F., Hallmann, R., Wendler, O., and Sorokin, L.M. (2001a). Endothelial cell laminin isoforms, laminins 8 and 10, play decisive roles in T cell recruitment across the blood-brain barrier in experimental autoimmune encephalomyelitis. J. Cell Biol. *153*, 933–946.

Sixt, M., Hallmann, R., Wendler, O., Scharffetter-Kochanek, K., and Sorokin, L.M. (2001b). Cell adhesion and migration properties of beta 2-integrin negative polymorphonuclear granulocytes on defined extracellular matrix molecules. Relevance for leukocyte extravasation. J. Biol. Chem. *276*, 18878–18887.

Sorokin, L., Sonnenberg, A., Aumailley, M., Timpl, R., and Ekblom, P. (1990). Recognition of the laminin E8 cell-binding site by an integrin possessing the alpha 6 subunit is essential for epithelial polarization in developing kidney tubules. J. Cell Biol. *111*, 1265–1273.

Steinman, R.M., Hawiger, D., and Nussenzweig, M.C. (2003). Tolerogenic dendritic cells. Annu. Rev. Immunol. *21*, 685–711.

Thyboll, J., Kortesmaa, J., Cao, R., Soininen, R., Wang, L., Iivanainen, A., Sorokin, L., Risling, M., Cao, Y., and Tryggvason, K. (2002). Deletion of the laminin alpha4 chain leads to impaired microvessel maturation. Mol. Cell. Biol. *22*, 1194–1202.

Ushiki, T., Ohtani, O., and Abe, K. (1995). Scanning electron microscopic studies of reticular framework in the rat mesenteric lymph node. Anat. Rec. *241*, 113–122.

Van Vliet, E., Melis, M., Foidart, J.M., and Van Ewijk, W. (1986). Reticular fibroblasts in peripheral lymphoid organs identified by a monoclonal antibody. J. Histochem. Cytochem. *34*, 883–890.

Vuento, M., and Vaheri, A. (1979). Purification of fibronectin from human plasma by affinity chromatography under non-denaturing conditions. Biochem. J. *183*, 331–337.

Witmer, M.D., and Steinman, R.M. (1984). The anatomy of peripheral lymphoid organs with emphasis on accessory cells: light-microscopic immunocytochemical studies of mouse spleen, lymph node, and Peyer's patch. Am. J. Anat. *170*, 465–481.

Witmer-Pack, M.D., Hughes, D.A., Schuler, G., Lawson, L., McWilliam, A., Inaba, K., Steinman, R.M., and Gordon, S. (1993). Identification of macrophages and dendritic cells in the osteopetrotic (op/op) mouse. J. Cell Sci. *104*, 1021–1029.

Zhang, H., Apfelroth, S.D., Hu, W., Davis, E.C., Sanguineti, C., Bonadio, J., Mecham, R.P., and Ramirez, F. (1994). Structure and expression of fibrillin-2, a novel microfibrillar component preferentially located in elastic matrices. J. Cell Biol. *124*, 855–863.